Nanotechnology **19** (2008) 405706 (6pp) doi:10.1088/0957-4484/19/40/405706

Internal structure of multiphase zinc-blende wurtzite gallium nitride nanowires

B W Jacobs[1], V M Ayres[1], M A Crimp[2] and K McElroy[1]

[1] Department of Electrical and Computer Engineering, Michigan State University, East Lansing, MI 48824, USA
[2] Department of Chemical Engineering and Materials Science, Michigan State University, East Lansing, MI 48824, USA

Received 3 June 2008, in final form 5 August 2008
Published 26 August 2008
Online at stacks.iop.org/Nano/19/405706

Abstract
In this paper, the internal structure of novel multiphase gallium nitride nanowires in which multiple zinc-blende and wurtzite crystalline domains grow simultaneously along the entire length of the nanowire is investigated. Orientation relationships within the multiphase nanowires are identified using high-resolution transmission electron microscopy of nanowire cross-sections fabricated with a focused ion beam system. A coherent interface between the zinc-blende and wurtzite phases is identified. A mechanism for catalyst-free vapor–solid multiphase nanowire nucleation and growth is proposed.

(Some figures in this article are in colour only in the electronic version)

1. Introduction

Semiconducting nanowires represent a new class of device building blocks with properties enhanced by their small size and large aspect ratios. Nanowires can be made from a variety of different semiconducting materials and therefore a wide assortment of band gaps, hole and electron mobilities, and mechanical properties are available for device engineering.

Gallium nitride nanowires in particular have received much attention due to their unique material properties. Gallium nitride (GaN) is a direct, wide band gap material [1]. It is capable of forming in the zinc-blende or wurtzite crystalline phases, further extending its versatility for device design. GaN nanowire optical and electronic devices, including lasers [2, 3], LEDs [4], UV detectors [5], and field effect transistors [6], and mechanical systems using a GaN nanowire as the primary device element [7] have been fabricated.

Nanowires must be of very high material purity, crystalline quality, and have tailored and reproducible crystallographic orientations to be viable in high performance devices. Plain-view high-resolution transmission electron microscopy (HRTEM) imaging with selective area electron diffraction (SAED) is a standard method for determining the crystal quality of as-grown semiconducting nanowires. It is, however, difficult to assess the internal nanowire structure using this method. The surface energy versus the volume total free energy contributions to the total nanowire free energy are differently proportioned than in bulk and can energetically enable complex internal structural arrangements [8, 9]. Such arrangements can lead to enhanced device properties, or induce defects which may significantly degrade device performance. Therefore, investigation of the internal structures of as-grown nanowires is important for both fundamental understanding and for successful nanodevice engineering [10–13].

The multiphase nanowire structures reported here incorporate highly crystalline zinc-blende and wurtzite phases simultaneously that extend in the longitudinal direction along the entire length of the nanowire [14]. The nanowires were synthesized in a quartz tube furnace at 850 °C in a direct reaction of gallium vapor and flowing ammonia (NH_3) [15–17]. Plain-view HRTEM (JEOL 2200FS, 200 kV) investigations of over 30 nanowires showed that the zinc-blende/wurtzite multiphase nanowires were consistently obtained using this growth method [18]. However, the internal orientation relationships that enable the multiphase structure could not be accurately assessed using plain-view HRTEM. Nanowire cross-sections, fabricated using a focused ion beam (FIB) system, proved important to identify details of the multiphase nanowire structure as they revealed internal crystallographic orientations that would be extremely difficult

to reconstruct from plain-view methods. In particular, all cross-sections of multiphase GaN nanowires examined to date have contained one or more coherent interfaces between zinc-blende {111} planes and wurtzite (0001) planes at domain interfaces. These coherent interfaces are considered to be important to the multiphase nanowire structure stability and growth.

2. Experimental details

2.1. Nanowire growth

GaN nanowires were grown in a tube furnace by reaction of gallium with ammonia as previously described in [15–17]. Gallium (99.999% purity/metals basis) was placed in a small BN boat (1 cm × 3 cm). The boat was placed into a 150 mm long 20 mm inside diameter quartz tube, which in turn was placed in the center of a 25 mm diameter, 1 m long quartz tube. The tubes and the BN boat were centered in a tube furnace. The 1 m process tube was sealed at both ends to form a vacuum system and evacuated by a two stage mechanical pump operating with Fromblin oil. The system was pumped down to a base pressure of ∼20 mTorr. An electronic mass flow controller then controlled the flow of electronic grade ammonia through the growth system. The flow rate was set between 80 and 90 sccm. A small valve at the end of the flow tube regulated the pressure in the system as measured by a capacitance manometer at the end of the process tube furthest from the pump. The furnace was rapidly ramped up to the 850 °C growth temperature. After 2 h, the furnace was turned off and cooled to ∼500 °C, at which point the ammonia flow was turned off and nitrogen substituted. When the system had cooled to room temperature, the inner quartz tube was removed and the GaN material removed. The width of the nanowires were between 60 and 150 nm and up to 500 μm in length.

2.2. FIB process

Cross-section TEM samples of the nanowires were fabricated using a FIB dual beam system (FEI Quanta 200 3D). The FIB was used to extract and mill nanowire samples until they were transparent to a TEM electron beam. For cross-section preparation, the nanowires and growth matrix were placed in ethanol and sonicated to free the nanowires from the matrix. The suspensions were then deposited on silicon wafers that had a layer of native oxide. A 5 nm titanium layer and 20 nm gold layer were thermally evaporated over the nanowires and substrate. These layers provided additional protection from ion beam damage in the initial phases of sample preparation. A thick layer of platinum, ∼4 μm, was deposited using reactive gas/ion interaction so that the nanowires would not be damaged during the ion milling process. The Pt/Au/Ti/nanowire/silicon layers were ion milled and extracted from the substrate using a micromanipulator and placed and secured on TEM grids using reactive gas/ion Pt deposition. The samples were milled further using the FIB so that they were thin enough to be transparent to the TEM electron beam.

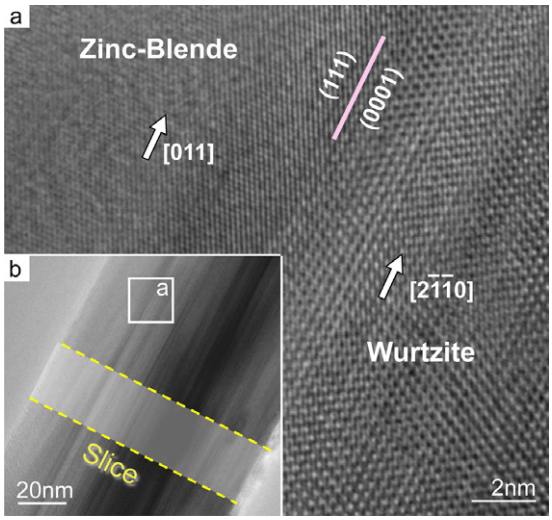

Figure 1. (a) A plain-view HRTEM image of the boxed area of the nanowire shown in (b), shows a coherent (111)/(0001) interface, indicated by the solid line, between the zinc-blende (ZB) and wurtzite (W) phases. The growth direction for each phase is also identified (arrows). (b) A plain-view TEM image of a typical multiphase nanowire. The dotted lines indicate where a cross-section might be taken.

3. Results and discussion

Figure 1(a) shows a typical plain-view HRTEM image of a multiphase nanowire. A very sharp interface with no observable defects between the zinc-blende and wurtzite phases is observed, indicated by the solid line. The nanowire growth is in the [011] direction for the zinc-blende phase and in the [2$\bar{1}\bar{1}$0] direction for the wurtzite phase, as determined by selected area electron diffraction (SAED) patterns, not shown. The sharp interface is identified as (111) zinc-blende/(0001) wurtzite, is a totally coherent interface, and extends the entire length of the nanowire. Figure 1(b) shows a typical TEM image of a multiphase nanowire and where a cross-section slice might be taken. Contrast variation in this image resulted not only from variations in thickness but also different crystalline phases. The white box indicates where the HRTEM image shown in figure 1(a) was taken.

Figure 2 shows details of the internal zinc-blende/wurtzite structure of a multiphase nanowire. The structure consisted of multiple zinc-blende and wurtzite domains in several orientations within the triangular nanowire. An HRTEM image of the multiphase GaN nanowire cross-section is shown in figure 2(a). The contrast variations seen in this image result from the multi-domain internal structure of the nanowire. The triangular cross-section is typical of the zinc-blende/wurtzite multiphase nanowire growth and consistent with previous AFM and SEM investigations. Platinum, gold and titanium metal layers deposited to protect the nanowire from ion beam damage during ion beam milling are labeled in the image. Figure 2(b) shows a sample midway through the extraction process in the FIB. Arrows in this figure indicate the silicon substrate and the Pt/Au/Ti protection layer covering the substrate and nanowire. The nanowire cross-section was

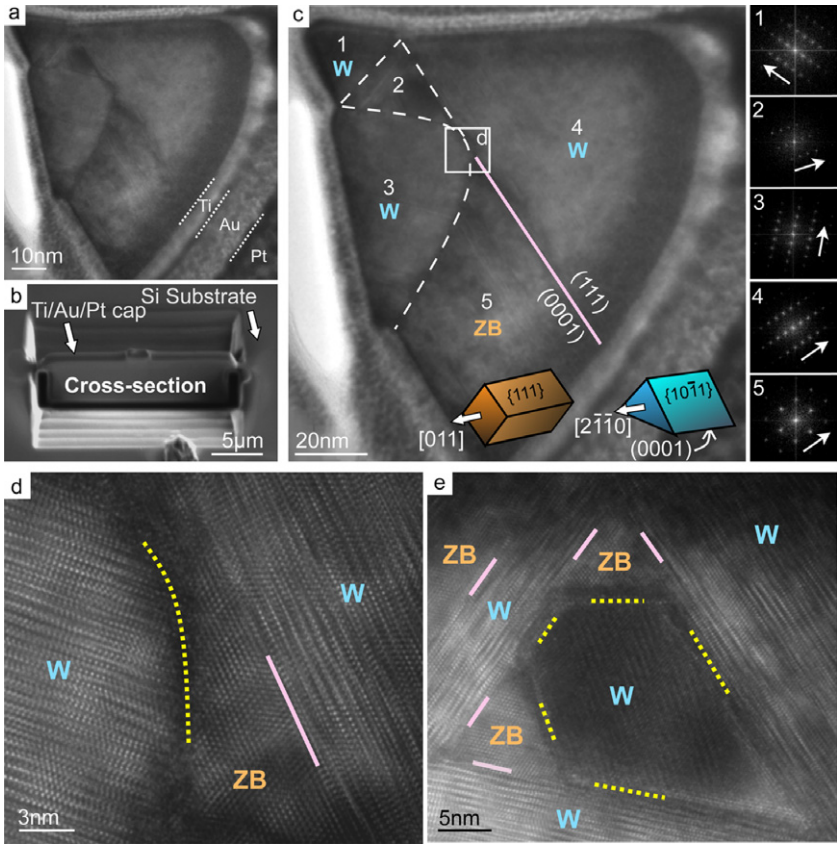

Figure 2. (a) HRTEM image of a multiphase GaN nanowire cross-section. Titanium, gold and platinum layers, labeled, were deposited before ion beam processing to protect the nanowire from ion beam damage. (b) An SEM image of a cross-section midway through the extraction process from the silicon substrate. (c) HRTEM image of the cross-section. The nanowire has 5 domains labeled 1–5. The solid line indicates a coherent interface. Corresponding FFTs shows the crystal orientations of the five domains. (d) HRTEM image of the boxed area in (c). The solid line indicates the coherent interface, and the dotted line an incoherent interface. The ababa stacking of the (0001) planes is clearly seen in this image, indicative of the wurtzite structure. (e) HRTEM image of domain 2. The solid lines indicate coherent interfaces and the dotted lines incoherent interfaces. The well-resolved lattices in the HRTEM images in (d) and (e) indicate the high crystal quality of each domain.

divided into five distinct crystallographic domains, indicated by the dashed lines, shown in figure 2(c). Fast Fourier transforms (FFTs) taken from HRTEM images of each domain show their corresponding crystallographic orientations. FFTs from domains 1–4 were indexed to the wurtzite structure along the [2$\bar{1}\bar{1}$0] zone axis, and the FFT from domain 5 was indexed to the zinc-blende structure along the [011] zone axis. These zone axes were consistent with the corresponding nanowire growth directions found in plain-view TEM studies, as shown in figure 1(a), and previously reported by our group [14]. Arrows in these FFTs are given to show the [0001] direction of the wurtzite domains and the [111] direction of the zinc-blende domain. The solid line indicates a long, ∼80 nm, totally coherent (111)/(0001) interface between zinc-blende domain 5 and wurtzite domain 4, that extended from the center of the nanowire to the outside edge.

The FFTs from each domain indicated that low energy facet planes corresponded to the external sides of the nanowire. In the zinc-blende domain 5, faceting occurred on the lowest energy {111} planes, resulting in the diamond-like shape with two exposed {111} planes and two {111} planes forming internal interfaces. In the wurtzite domains, external faceting occurred on the {10$\bar{1}$1} planes. Each individual wurtzite domain was triangular in shape, with the (0001) planes making up one side of each triangle. It was noted that the (0001) planes were observed to terminate only as internal interfaces.

Figure 2(d) displays an enlarged view of the boxed area in figure 2(c). The coherent interface, indicated by the solid line between the internal (0001) and (111) planes (confirmed by FFTs taken from the corresponding areas), had atomic registry with no observable defects. The second interface between zinc-blende domain 5 and wurtzite domain 3 was incoherent, indicated by the dotted line.

Figure 2(e) displays a close-up of domain 2 and shows a dark contrast wurtzite domain in the center. Two resolvable triangular zinc-blende domains on the left and top of the dark contrast wurtzite domain were observed (a possible third zinc-blende area on the lower right side was too small to resolve). The two zinc-blende domains formed coherent interfaces with the surrounding wurtzite domains, indicated by solid lines in figure 2(e). The dark wurtzite domain formed incoherent interfaces with the two zinc-blende domains, as well as with the surrounding wurtzite domains, indicated by the dotted lines.

The multiphase nanowires grew from a matrix of GaN platelets [14, 15]. An SEM image, shown in figure 3(a), shows typical features of the GaN platelet matrix that formed

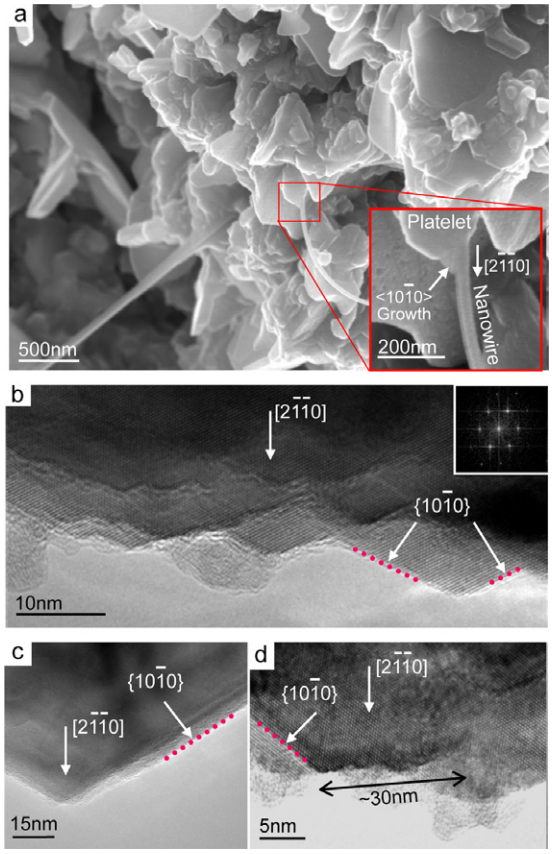

Figure 3. (a) SEM image of the GaN growth matrix. Typical platelets and two nanowires that nucleated from platelets can be seen. The inset is a close-up of the indicated area. Competitive step-ledge growth along the $\langle 10\bar{1}0\rangle$ direction is indicated by the arrow. (b) HRTEM of the side of a platelet. Dotted lines indicate the $\{10\bar{1}0\}$ sides of the ledges. An FFT, shown in the inset, confirms the orientation of the ledges, and corresponds to the wurtzite structure along the [0001] zone axis. (c) HRTEM image of smooth platelet side. (d) HRTEM image of an individual nanoscale ledge. The $(2\bar{1}\bar{1}0)$ planes are exposed as indicated by the double arrow.

at 850 °C. Relatively uniform platelets with sizes between 200 nm and 1 μm were observed. Two nanowires that nucleated from the matrix can be seen in this image. A close-up of the smaller nanowire with $\langle 2\bar{1}\bar{1}0\rangle$ growth orientation is shown in the inset. Evidence of a competitive growth along the $\langle 10\bar{1}0\rangle$ direction is indicated by the arrow in this figure. Quantitative EDS and SAED patterns, not shown, confirmed that the platelets were GaN. Figures 3(b) and (c) are HRTEM images of platelet sides. A network of nanoscale ledges was found to form on some sides, as shown in figure 3(b), while other sides were smooth with surface variations of less than 1 nm, as shown in figure 3(c). An FFT, shown in the inset of figure 3(b), shows the orientation of the nanoscale ledges, confirms that they were in the same orientation and coherent with the platelet, and identifies them as wurtzite. When present, the nanoscale ledges were roughly 20–30 nm wide and about 20–30 nm thick, as inferred from the electron transparency of each nanoscale ledge. Nanoscale ledges could be intact as shown in figure 3(b) or show evidence of decomposition, as shown in figure 3(d). Exposed $\{2\bar{1}\bar{1}0\}$ planes can be seen in this image, denoted by the double arrow.

Results of the SEM and TEM matrix investigations suggest these multiphase GaN nanowires grow by way of a catalyst-free, vapor–solid mechanism. The nanoscale ledges, found on the sides of GaN wurtzite platelets as reported here, are likely to play an important role in nanowire nucleation. The HRTEM image shown in figure 3(d), shows evidence of a nanoscale ledge with exposed the $\{2\bar{1}\bar{1}0\}$ planes. These planes are expected to be highly active sites, and they correspond to the wurtzite domain growth orientation, $\langle 2\bar{1}\bar{1}0\rangle$, which is the fastest growth direction in wurtzite GaN thin films. The nanoscale ledge areas are also similar in width to the individual wurtzite domains found in the nanowire cross-sections, 20–30 nm, as indicated by their electron transparency (comparison of figure 2(c) with figures 3(b)–(d)). Networks of nanoscale ledges were identified, as shown in figure 3(b). These networks could have multiple neighboring nanoscale ledge sites with active exposed $\langle 2\bar{1}\bar{1}0\rangle$ planes. Wurtzite domain nucleation from neighboring sites may explain the multiple wurtzite domains found in these nanowires. In a vapor–solid mechanism, competitive step-ledge nucleation would be expected on the nanoscale ledge $\{10\bar{1}0\}$ faces. The $\langle 10\bar{1}0\rangle$ direction is the second fastest growth direction in wurtzite GaN thin films. Structures near the primary nanowire nucleation sites that grew in the $\langle 10\bar{1}0\rangle$ direction were typically observed for nanowires grown at 850 °C, as shown in the inset in figure 3(a). The typical nanowires shown in figure 3(a) indicate that $\langle 2\bar{1}\bar{1}0\rangle$ growth eventually dominates in these nanowires. The $\langle 0001\rangle$ direction is the third fastest growth direction in wurtzite GaN thin films. Evidence of $\langle 0001\rangle$ orientation nanowire growth at higher growth temperatures will be reported in a separate publication.

In this paper and previous work [14], we have reported evidence that zinc-blende growth in multiphase nanowires occurs. We have not seen evidence for a separate zinc-blende domain nucleation site to date. As of now, the evidence reported here and previously reported evidence by other groups, suggest two possible explanations for the formation of the zinc-blende phase. First, lattice-mismatched nucleation of zinc-blende $\langle 011\rangle$ oriented GaN nanowire domains on the wurtzite GaN substrate may occur. Lattice-mismatched hetero-epitaxial growth of nanowires has been reported. Examples include $\langle 0001\rangle$ oriented GaN nanorods [19] and nanowires [20, 21] grown on c-sapphire substrates by molecular beam epitaxy, $\langle 0001\rangle$ oriented ZnO nanowires grown on (111) silicon substrates by vapor phase epitaxy [22] and $\langle 112\rangle$ oriented ZnSe nanowires grown on (001) silicon substrates by metal–organic chemical vapor deposition [23]. Second, multiphase GaN nanowire growth may be stabilized by the formation of the coherent zinc-blende/wurtzite interface that renders maintenance of the multiphase configuration energetically attractive. Instability of the (0001) surfaces in wurtzite GaN, resulting in multiple surface reconstructions especially for the nitrogen-terminated polarity, is known from thin film studies [24, 25]. Possible evidence for wurtzite (0001) plane stabilization, through formation of the coherent interface with the non-polar zinc-blende {111} planes, is seen in the multiphase nanowire cross-section reported here. Each wurtzite domain is triangular with external faceting only on

the $\{10\bar{1}1\}$ planes. The (0001) planes in each domain are all internal planes. An internal (0001) terminating plane may use the zinc-blende structure as a way to avoid exposing an unstable surface through the formation of a coherent interface and complete transition to the zinc-blende phase. This may be the case for the transition between the wurtzite domain 4 and zinc-blende domain 5 shown in figure 2(c). In certain instances the zinc-blende phase may also act as an option to fill awkward gaps in the nanowire, as seen in figure 2(e), where two triangular zinc-blende domains formed coherent interfaces with the surrounding wurtzite domains.

There are device implications associated with the internal structure of the zinc-blende/wurtzite multiphase GaN nanowires. Multiphase nanowires based on longitudinal phase separation in heterostructures and now in homostructures, as reported here and previously [14], represent a new class of waveguide structures. Important applications in quantum transport and phase-specific transport could also be developed based on this structure. We have previously reported measurements of high current density transport in these multiphase GaN nanowires [26]. The possible development of an energy landscape at the polar wurtzite/non-polar zinc-blende coherent interface, which may effectively confine carriers, is currently under investigation by our group. Incoherent interfaces between wurtzite–zinc-blende and wurtzite–wurtzite domains are also reported here. A purely wurtzite nanowire with incoherent domains not stabilized by zinc-blende phases would be expected to have multiple defects that would affect its electronic/opto-electronic device performance.

4. Conclusion

In summary, a nanowire cross-section fabricated with a FIB system was analyzed with HRTEM. A novel multiphase gallium nitride nanowire internal structure, with multiple zinc-blende and wurtzite crystalline domains that grow simultaneously that extend along the entire length of the nanowire, was observed. Coherent {0001}/{111}interfaces between the zinc-blende and wurtzite phases were identified. A growth mechanism was proposed. The electronic/mechanical effects of the zinc-blende phase are under investigation.

Acknowledgments

The support of NASA Goddard Space Flight Center, MEI Task No. 14, and the National Science Foundation IREE program DMI-0637134 are gratefully acknowledged. The authors thank Maoqi He and Joshua B Halpern of Howard University for sourcing the nanowires used in this study. One author (BWJ) would like to thank the NASA Graduate Student Researchers Program. The FIB cross-sections were fabricated at the Electronic Microbeam Analysis Laboratory (EMAL) at the University of Michigan.

References

[1] Bougrov V, Levinshtein M E, Rumyantsev S L and Zubrilov A 2001 *Properties of Advanced Semiconductor Materials GaN, AlN, InN, BN, SiC, SiGe* (New York: Wiley) pp 1–30

[2] Greytak A B, Barrelet C J, Li Y and Lieber C M 2004 Semiconductor nanowire laser and nanowire waveguide electro-optic modulators *Appl. Phys. Lett.* **87** 151103

[3] Johnson J C, Choi H-J, Knutsen K P, Schaller R D, Yang P and Saykally R J 2002 Single gallium nitride nanowire lasers *Nat. Mater.* **1** 106–10

[4] Kim H-M, Kang T W and Chung K S 2003 Nanoscale ultraviolet-light-emitting diodes using wide-bandgap gallium nitride nanorods *Adv. Mater.* **15** 567–9

[5] Han S, Jin W, Zhang D, Tang T, Li C, Liu X, Liu Z, Lei B and Zhou C 2004 Photoconduction studies on GaN nanowire transistors under UV and polarized UV illumination *Chem. Phys. Lett.* **389** 176–80

[6] Huang Y, Duan X, Cui Y and Lieber C M 2002 Gallium nitride nanowire nanodevices *Nano Lett.* **2** 101–4

[7] Nam C Y, Jaroenapibal P, Tham D, Luzzi D E, Evoy S and Fischer J E 2006 Diameter-dependent electromechanical properties of GaN nanowires *Nano Lett.* **6** 153–8

[8] Diao J, Gall K and Dunn M L 2003 Surface-stress-induced phase transformation in metal nanowires *Nat. Mater.* **2** 656–60

[9] Bierman M J, Lau Y K A, Kvit A V, Schmitt A L and Jin S 2008 Dislocation-driven nanowire growth and Eshelby twist *Science* **320** 1060–3

[10] Jiang X, Xiong Q, Nam S, Qian F, Li Y and Lieber C M 2007 InAs/InP radial nanowire heterostructures as high electron mobility devices *Nano Lett.* **7** 3214–18

[11] Mikkelsen A, Sköld N, Ouattara L, Borgström M, Andersen J N, Samuelson L, Seifert W and Lundgren E 2004 Direct imaging of the atomic structure inside a nanowire by scanning tunnelling microscopy *Nat. Mater.* **3** 519–23

[12] Tham D, Nam C Y and Fischer J E 2006 Defects in GaN nanowires *Adv. Funct. Mater.* **16** 1197–202

[13] Tao X and Li X 2008 Catalyst-free synthesis, structural, and mechanical characterization of twinned $Mg_2B_2O_5$ nanowires *Nano Lett.* **8** 505–10

[14] Jacobs B W, Ayres V M, Petkov M P, Halpern J B, He M, Baczewski A D, McElroy K, Crimp M A, Zhang J and Shaw H C 2007 Electronic and structural characteristics of zinc-blende wurtzite biphasic homostructure GaN nanowires *Nano Lett.* **7** 1435–8

[15] He M, Zhou P, Mohammad S N, Harris G L, Halpern J B, Jacobs R, Sarney W L and Salamanca-Riba L 2001 Growth of GaN nanowires by direct reaction of Ga with NH_3 *J. Cryst. Growth* **231** 357–65

[16] He M, Minus I, Zhou P, Mohammad S N, Halpern J B, Jacobs R, Sarney W L, Salamanca-Riba L and Vispute R D 2000 Growth of large-scale GaN nanowires and tubes by direct reaction of Ga with NH_3 *Appl. Phys. Lett.* **77** 3731–3

[17] El Ahl A M S, He M, Zhou P, Harris G L, Salamanca-Riba L, Felt F, Shaw H C, Sharma A, Jah M and Lakins D 2003 Systematic study of effects of growth conditions on the (nano-, meso-, micro) size and (one-, two-, three-dimensional) shape of GaN single crystals grown by a direct reaction of Ga with ammonia *J. Appl. Phys.* **94** 7749–56

[18] Ayres V M *et al* 2006 Investigations of heavy ion irradiation of gallium nitride nanowires and nanocircuits *Diamond Relat. Mater.* **15** 1117–21

[19] Kuo S Y, Kei C C, Chao C K, Hsiao C N, Lai F-I, Kuo H C, Hsieh W F and Wang S C 2005 *Proc. 2005 5th IEEE Conf. on Nanotech. (Nagoya)*

[20] Geelhaar L, Chèze C, Weber W M, Averbeck R, Riechert H, Kehagias T, Komninou P, Dimitrakopulos G P and Karakostas T 2007 Axial and radial growth of Ni-induced GaN nanowires *Appl. Phys. Lett.* **91** 093113

[21] Lari L, Murray R T, Bullough T J, Chalker P R, Gass M, Chèze C, Geelhaar L and Riechert H 2008 Nanoscale

compositional analysis of Ni-based seed crystallites associated with GaN nanowire growth *Physica* E **40** 2457–61

[22] Park W I, Yi G-C, Kim M and Pennycook S J 2002 ZnO nanoneedles grown vertically on Si substrates by non-catalytic vapor-phase epitaxy *Adv. Mater.* **14** 1841–3

[23] Zhang X T, Liu Z, Leung Y P, Li Q and Hark S K 2003 Growth and luminescence of zinc-blende structured ZnSe nanowires by metal–organic chemical vapor deposition *Appl. Phys. Lett.* **83** 5533–5

[24] Rapcewicz K, Nardelli M B and Bernholc J 1997 Theory of surface morphology of wurtzite GaN(0001) surfaces *Phys. Rev.* B **56** R12725–8

[25] Fritsch J, Sankey O F, Schmidt K E and Page J B 1998 *Ab initio* calculation of the stoichiometry and structure of the (0001) surfaces of GaN and AlN *Phys. Rev.* B **57** 15360–71

[26] Jacobs B W, Ayres V M, Stallcup R E, Hartman A, Tupta M A, Baczewski A D, Crimp M A, Halpern J B, He M and Shaw H C 2007 Electron transport in zinc-blende wurtzite biphasic gallium nitride nanowires and GaNFETs *Nanotechnology* **18** 475710